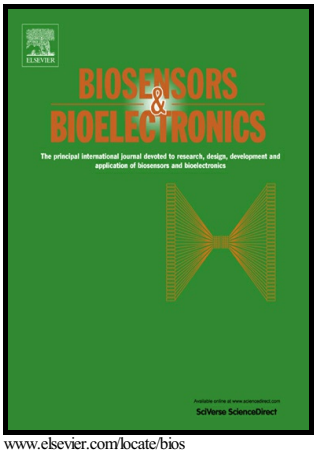

www.elsevier.com/locate/bios

Hierarchical $CuInS_2$-Based Heterostructure: Application for Photocathodic Bioanalysis of Sarcosine

Xin-Yuan Jiang, Ling Zhang, Yi-Li Liu, Xiao-Dong Yu, Yan-Yu Liang, Peng Qu, Wei-Wei Zhao, Jing-Juan Xu, Hong-Yuan Chen

PII: S0956-5663(18)30133-7
DOI: https://doi.org/10.1016/j.bios.2018.02.039
Reference: BIOS10301

To appear in: *Biosensors and Bioelectronic*

Received date: 27 December 2017
Revised date: 13 February 2018
Accepted date: 14 February 2018

Cite this article as: Xin-Yuan Jiang, Ling Zhang, Yi-Li Liu, Xiao-Dong Yu, Yan-Yu Liang, Peng Qu, Wei-Wei Zhao, Jing-Juan Xu and Hong-Yuan Chen, Hierarchical $CuInS_2$-Based Heterostructure: Application for Photocathodic Bioanalysis of Sarcosine, *Biosensors and Bioelectronic,* https://doi.org/10.1016/j.bios.2018.02.039

Hierarchical $CuInS_2$-Based Heterostructure: Application for Photocathodic Bioanalysis of Sarcosine

Xin-Yuan Jiang[a,1], Ling Zhang[a,b,c,1], Yi-Li Liu[d], Xiao-Dong Yu[,a], Yan-Yu Liang[*,b], Peng Qu[*,d], Wei-Wei Zhao[*,a], Jing-Juan Xu[a] and Hong-Yuan Chen[a]*

[a]State Key Laboratory of Analytical Chemistry for Life Science and Collaborative Innovation Center of Chemistry for Life Science, School of Chemistry and Chemical Engineering, Nanjing University, Nanjing 210023, China.

[b]School of Materials Science and Technology, Nanjing University of Aeronautics and Astronautics, Nanjing 211106, China.

[c]School of Material and Chemical Engineering, Bengbu College, Bengbu 233000, China.

[d]Henan Key Laboratory of Biomolecular Recognition and Sensing, College of Chemistry and Chemical Engineering, Shangqiu Normal University, Shangqiu 476000, China.

[1]These authors contributed to this work equally.

* Corresponding authors.
E-mail addresses: yuxd@nju.edu.cn (X.-D. Yu), liangyy403@126.com (Y.-Y. Liang), qupeng0212@163.com (P. Qu), zww@nju.edu.cn (W.-W. Zhao)

ABSTRACT: In this study, on the basis of hierarchical $CuInS_2$-based heterostructure, a novel cathodic photoelectrochemical (PEC) enzymatic bioanalysis of the sarcosine detection was reported. Specifically, heterostructured $CuInS_2$/NiO/ITO photocathode was prepared and sarcosine oxidases (SOx) were integrated for the construction of the enzymatic biosensor. In the bioanalysis, the O_2-dependent suppression of the cathodic photocurrent can be observed due to the competition between the as-fabricated O_2-sensitive photocathode and the SOx-catalytic event toward O_2 reduction. Based on the sarcosine-controlled O_2 concentration, a novel photocathodic enzymatic biosensor could be realized for the sensitive and specific sarcosine detection. This work manifested the great potential of $CuInS_2$-based heterostructure as a novel platform for future PEC bioanalytical development and also a PEC method for sarcosine detection, which could be easily extended to numerous other enzymatic systems and to our knowledge has not been reported. This work is expected to stimulate more interest in the design and implementation of numerous $CuInS_2$-based heterostructured photocathodic enzymatic sensing.

KEYWORDS: Photoelectrochemical, Bioanalysis, $CuInS_2$, Heterostructure, Sarcosine Oxidase

1. Introduction

Photocathodes, which are used in photoelectrochemical (PEC) water splitting, have been shown to be applicable in the development of PEC bioanalysis, which represents a newly emerged field of novel bioanalysis (Zhang et al., 2012; Wang et al., 2015;Zhao et al., 2014; Zhang et al., 2017). This was realized by replacing H_2O or H^+ reduction with the reduction of an appropriate electron acceptor (e.g. dissolved O_2) in the electrolyte. One significant advantage of photocathodic bioanalysis is its good anti-interference capability against reductive substances and thus more suitable for the detection of complex biological samples. This is because photocathodes are prone to interact with electron acceptors more than electron donors (e.g., ascorbic acid, glutathione, dopamine, and nicotinamide adenine dinucleotide that coexist in the biological samples) in the electrolyte (Wang et al., 2014; Surbi et al., 2012; Wang et al., 2015). Unfortunately, despite their fascinating features, the research in this field lags far behind its counterpart of the photoanodic bioanalysis. Comparing with the application of photoanodes, there has only been a paucity of studies that explore the photocathode for novel PEC bioanalysis (Takahashi et al., 2010; Zang et al., 2016;Dai et al., 2017). For example, Wang et.al first utilized the p−type PbS quantum dots (QDs) for versatile PEC DNA analysis and aptasensing (Wang et al., 2015; Wang et al., 2015) .

Hierarchical heterostructures, assembled by low-dimensional building blocks, e.g., particles, wires, rods, tubes, cones or sheets, have been among the most important research hotspots in the past years due to their unique characteristics and manifold implications in various fields (Mai et al., 2011; Ostermann et al., 2006; Zhang et al., 2005; Shen et al., 2006; Jaffar et al., 2004; Peng et al., 2014; Zhu et al., 2012; Ruan et al., 2017; Zhu et al., 2017). In the quest for achieving better semiconducting performances, hierarchical heterostructures consisting of different

semiconductors are being considered as favorite schemes as compared to the pure ones. It is believed that the such a structure could integrate different properties of the individual semiconductors and thus generate enhanced properties (Zhou et al., 2013; Mai et al., 2011; Wang et al., 2009). Specifically, the appropriate arrangement of particular semiconductors makes possible the construction of desirable photoelectrodes and therein contribute to the photoinduced charge separation in both the semiconductors and inhibit the charge recombination, resulting in the enhancement in photocurrent generation. In this respect, numerous anodic heterojunctions have been implemented in previous PEC bioanalysis (Zhang et al., 2016; Han et al., 2017). For instance, Zhang proposed a simultaneous PEC immunoassay of dual cardiac markers on the basis of the CdS quantum dots functionalized TiO_2 nanotubes electrodes. Expectedly, appropriate alignment of particular p-type semiconductors could also produce novel heterojunction photocathodes with fascinating characteristics for advanced PEC bioanalysis.

Copper indium disulfide ($CuInS_2$) represents a promising direct semiconductor with a band gap in the visible region (Eg = 1.5 eV), a large optical absorption coefficient ($\alpha > 105$ cm^{-1}), high photostability, and pronounced defect tolerance (Guo et al., 2009; Li et al., 2010; Li et al., 2010; Kuo et al., 2009). As an attractive ternary p-type semiconductor, $CuInS_2$ has been intensively studied for applications in many fields such as photocatalysis, solar energy conversion, photodetectors, light-emitting devices, and biomedical applications (Kolny et al., 2013; Yue et al., 2010; Yong et al., 2010; Huang et al., 2012). However, its utilization in the field of PEC bioanalysis has seldom been studied. Very recently, Fan et al. reported the very example of using the $CuInS_2$ modified ITO to conduct the PEC immunoassay of prostate-specific antigen (Fan et al., 2016). However, $CuInS_2$-based heterostructure has yet to be exploited in the field of PEC bioanalysis. Different from $CuInS_2$, NiO is a large band gap (3.6–4.0 eV) p-type

semiconductor that mainly adsorbs ultraviolet light (Niklasson et al., 2007). Recently, sensitized NiO based photoelectrode has also drawn more attention because of its desired efficiency, high availability, and balanced economics (Brown et al., 2016; Yang et al., 2011; Ji et al., 2013). Obviously, small band gap $CuInS_2$ integrated with large band gap NiO may present a novel p-p heterojunction electrode for advanced PEC bioanalysis development.

Sarcosine, also known as *N*-methylglycine, is a naturally occurring nontoxic amino acid, which is ubiquitous in biological materials and is present in many foods such as egg yolks, ham, vegetables, etc (Willsey et al., 2015; Kopper, 1950; Wyss et al., 2000; Wang et al., 2013). In human body, it is an important intermediate and byproduct in glycine synthesis/degradation, and has been investigated in relation to the mental illness schizophrenia (Tsai et al., 2004). Further research has demonstrated that sarcosine might be a potential biomarker for the prostate cancer (PCa), and its levels seemed to control the invasiveness of this disease (Sreekumar et al., 2009). Quantitative determination of sarcosine is thus important, and can be generally achieved by various mass-spectrometry (MS) based techniques, e.g. high performance liquid-chromatography-MS (HPLC-MS) and gas-chromatography–MS (GC–MS) (Gray et al., 2017; Meyer et al., 2011; Jiang et al., 2010). Nevertheless, these methods are costly and necessitate cumbersome operation and sample preparation processes, rendering them inappropriate for wider routine detection. To overcome these shortcomings, analytical chemists have exploited the electrochemistry-based techniques to detect the electrochemically inactive sarcosine. For example, many amperometric and impedimetric protocols have been proposed (Xue et al., 2017). Amid various strategies, the most popular approach is to monitor the enzymatic generation of H_2O_2 by the use of sarcosine oxidase (SOx), which, with the aid of ambient O_2, can catalyze the oxidative demethylation of sarcosine to glycine, formaldehyde, H_2O_2. So the indirect detection of

sarcosine can be realized by electrochemical detection of H_2O_2 (Rebelo et al., 2014). Especially, as advanced electrochemical techniques, electrochemiluminescence (ECL) and PEC bioanalysis have also been investigated toward this purpose. For example, Prodi et al. has reported an interesting ECL-supramolecular approach for sarcosine analysis, in which the sarcosine acted as co-reagent in a $Ru(bpy)_3^{2+}$-ECL process (Valenti et al., 2015). Lisdat et al. has realized the exquisite PEC sarcosine analysis with the use of CdSe/ZnS quantum dots (QDs) (Riedel et al., 2013). Despite the efforts in these two reports, the exploitation using the advanced ECL or PEC techniques is indeed quite limited, as compared to the MS-based or traditional electrochemical-based techniques.

In this work, we describe a novel photocathodic bioanalysis toward sarcosine detection on the basis of SOx modified $CuInS_2$-based heterostructure electrode. Specifically, $CuInS_2$ microspheres ($CuInS_2$ MSs) and nanoporous 3D NiO/indium tin oxide (ITO) were both obtained via the hydrothermal synthesis and then coupled as the p-p heterojunction electrode (Scheme 1). After the SOx immobilization, the constructed enzyme sensor was applied for the PEC bioanalysis of sarcosine, in the process of which the O_2-dependent suppression of the cathodic photocurrent can be observed due to the competition between the as-fabricated O_2-sensitive photocathode and the SOx-catalytic event toward O_2 reduction.

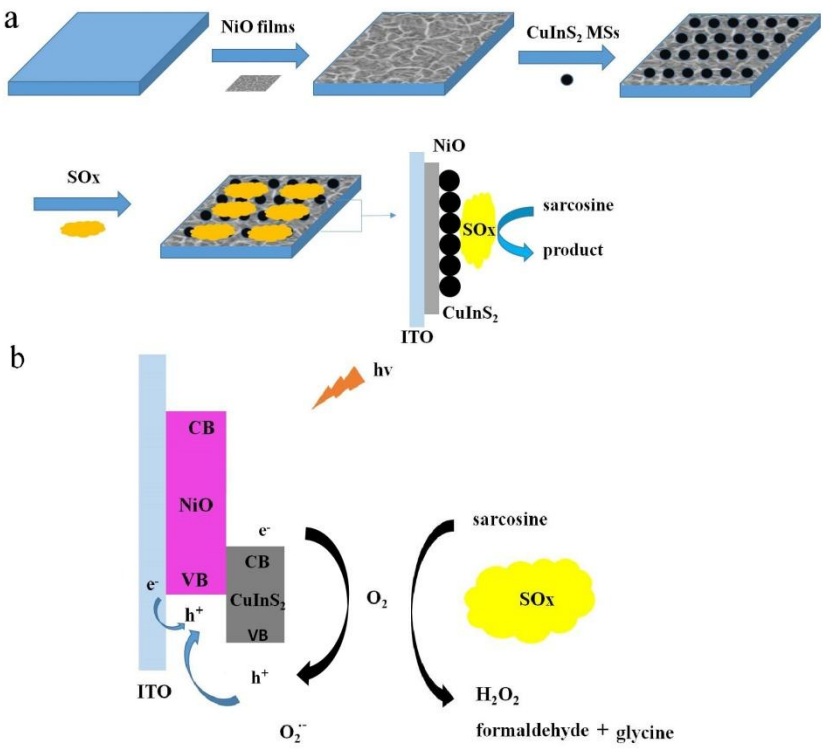

Scheme 1 (a) Preparation of SOx/$CuInS_2$/NiO/ITO electrode and the application for the PEC bioanalysis of sarcosine and (b) Operation principle of the PEC sensor

This was a novel and sensitive photocathodic sarcosine biosensor and exhibited good performance toward sarcosine detection. The work manifested the great potential of $CuInS_2$-based heterostructure as a novel platform for future PEC bioanalytical development and also a sensitive method for photocathodic sarcosine detection, which could be easily extended to numerous other enzymatic systems and to our knowledge has not been reported. The detailed fabrication, characterization, and performance of the developed $CuInS_2$-based cathodic PEC sarcosine biosensor are described below.

2. Experimental section

2.1. Reagents and Apparatus. All chemical reagents were supplied from Sigma-Aldrich, Alfa Aesar, Sunshine, Nanjing Chemical Reagent Co., Ltd. and Sinopharm Chemical Reagent Co., Ltd, and were used without further purification. Poly(diallyldimethylammonium chloride) (PDDA, 20%, w/w in water, MW = 200 000-350 000) were supplied from Sigma-Aldrich, (St. Louis, MO). Sarcosine oxidase (Sox, 10kU) were supplied from Bioss Co., Ltd(China). D-(+)-glucose, ascorbic acid (AA), urea, L-histidine, L-lysine, Potassium hydroxide were supplied from Sinopharm Chemical Reagent Co., Ltd (China). Nickel nitrate was supplied from Strem Chemicals, Inc. CuCl, $InCl_3$, ethylene, glycol, ethylene, examethylene tetramine (HETA) and thiourea (H_2NCSNH_2) were supplied from Nanjing Chemical Reagent Co., Ltd. The indium tin oxide (ITO) glass (type N-STN-S1-10 with ITO coating 180±20 nm, sheet resistance 8.1± 0.6 Ω cm^{-2}) was obtained from China Southern Glass Holding Co., Ltd., Shenzhen, China.

Ultrapure water (18.2 MΩ·cm resistivity at 25 °C, Millier Q) was used in all experiments. SEM images were recorded by a Hitachi S4800 scanning electron microscope (Hitachi Co., Japan). XPS was obtained from PHI 5000 VersaProbe (UlVAC-PHI Co., Japan). The UV-vis absorption spectra and UV−vis diffuse reflectance spectra were obtained on a Shimadzu UV-3600 UV-vis-NIR spectrophotometer (Shimadzu Co., Japan). XRD spectra were characterized by powder X-ray diffraction (XRD) [X'TRA, Cu Kα (ARL Co.)].

PEC measurements were performed with a homemade PEC system equipped with a 5 W light-emitting diode lamp emitting at around 415 nm with a power density of 1.6 mW/cm^2. The photocurrent was measured on a CHI 660C electrochemical workstation with a three-electrode system: a $CuInS_2$/NiO/ITO electrode with a geometrical circular area (0.5 cm in diameter) as the working electrode, a Pt wire as the counter electrode, and a saturated Ag/AgCl electrode as the

reference electrode. The photocurrent measurements were taken at a constant potential of 0.0 V (vs saturated Ag/AgCl), and 0.1 M phosphate buffer (pH 7.4) was used as the supporting electrolyte for photocurrent measurements.

2.2. Synthesis of $CuInS_2$. The fabrication of CuInS2 was according to previous report (Fan et al., 2016). 0.015 mol CuCl, 0.015 mol $InCl_3$ and 0.06 mol H_2NCSNH_2 were dissolved in 20 ml ethylene glycol with fierce stir. Then the solution was transferred into a 50 mL of tightly sealed Teflon-lined autoclave. The above solution was kept at 200 °C for 24 h, the black sediments of $CuInS_2$ MSs were obtained by centrifugation. The as-obtained products were washed with ethanol and ultrapure water several times and then dried at 100 °C over night to acquire power products.

2.3. Assemble of NiO/ITO electrodes. Nanoporous NiO films were fabricated on ITO-coated glass substrates using hydrothermal method. The ITO slices were cleaned by immersion in boiling 2.0 M KOH 2-propanol solution for 20 min, followed by washing copiously with ultrapure water and dried at 80 °C. Then the ITO slices were further cleaned by piranha solution, followed by washing thoroughly with ultrapure water and dried at 80 °C. For the hydrothermal method, the reaction solution was aqueous which containing 0.25 M $Ni(NO_3)_2{\cdot}6H_2O$ and 0.25 M HETA. The above solution was transferred into a vial and the ITO electrodes were placed at the bottom of the vial. The vial was then heated in an oven at 90°C for 10 min. Then the ITO was washed with ultrapure water for about 10 times, dried and heated to 300 °C in air for 30 min.

2.4. Fabrication of $CuInS_2$/NiO/ITO Photocathode. The $CuInS_2$/NiO/ITO electrode was fabricated by dripping the $CuInS_2$ solution (12 mg in 2 ml ultrapure water) onto the NiO/ITO electrode. After dried under 80℃, the electrode was heated to 160℃ in air for 2h.

2.5. Development of SOx Biosensor. SOx was bioconjugated onto the $CuInS_2$/NiO/ITO electrode by immersing the $CuInS_2$/NiO/ITO electrode into the SOx solution (0.1 mg/mL) for 30 min, then the electrode was carefully washed with ultrapure water and a monolayer of SOx was modified on the $CuInS_2$/NiO/ITO electrode.

3. Results and discussions

3.1. Structural Characterization. NiO is a low-cost p-type large band gap (3.6–4.0 eV) semiconductor which mainly adsorbs ultraviolet light and can be easily fabricated by multiple methods (Niklasson et al., 2007). Currently, sensitized NiO based photocathode is a new field of investigation with increasing scientific interest due to its high accessibility, balanced economics, and desired efficiency. Especially, a three-dimensional (3D) nanoporous NiO structure with high specific surface area would be more advantageous for the loading of a large amounts of sensitizers. On the other hand, $CuInS_2$ is an attractive less-toxic alternative to Cd- or Pb-based QDs with high absorption coefficient ($\sim 10^5$ cm^{-1}) and near-optimal bulk band gap energy (1.5 eV) (Guo et al., 2009; Li et al., 2010; Li et al., 2010; Kuo et al., 2009).

Inspired by their intriguing properties, of particular interest here is the possibility of integrating $CuInS_2$ with the 3D porous NiO nanofilms to exploit the innovative heterostructure photocathode toward advanced PEC bioassay application. The success of which can provide great opportunities for further development of new signaling strategies as well as the implementation of novel PEC bioanalytical devices.

NiO nanofilm was fabricated on the ITO glass using the aforementioned hydrothermal method (Lepleux et al., 2009). And its morphology was then revealed by SEM (Figure 1A). Obviously, the as-fabricated nanostructured NiO thin film exhibited a highly crossed three-

dimensional (3D) porous architecture that composed of densely interconnected nanoflakes. These nanoflakes have lateral dimension in the micrometer size, height of several hundred nm. This structure could provide great surface area for the subsequent loading of guest species $CuInS_2$ microspheres and also be advantageous to the efficient charge separation and transfer of the photogenerated electron-hole pairs. The crystal structure of the as-deposited NiO nanofilm was further identified by XRD. Quantitative analysis of the pattern would index all the observed peaks to the face-centered cubic NiO (JCPDS:78-0643, with characteristic peaks of the NiO at 2θ = 37.26°, 43.28°, 62.76°, 75.28° corresponding to the (111), (200), (220) and (311) crystal planes of cubic NiO, respectively), suggesting that no Ni related impurities exist in the sample (Figure 1B). The SEM image of the as synthesized $CuInS_2$ microspheres showed they appeared as spherical particles with numerous tiny nanoparticles (Figure 1C). In the XRD pattern of the $CuInS_2$, the observed peaks were assigned to diffractions from the (112), (004), (220/204), (312) and (332) crystal faces, which is in accordance with monoclinic $CuInS_2$ [JCPDS:27-0159] (Figure 1D). It was observed that all the peaks were very prominent and sharp, indicating that the product had a relatively good crystallinity. The SEM image of synthesized $CuInS_2$/NiO electrode revealed that $CuInS_2$ were fixed on NiO firms (Figure 1E) and the the XRD pattern of the $CuInS_2$/NiO electrode also confirmed it (Figure 1F).

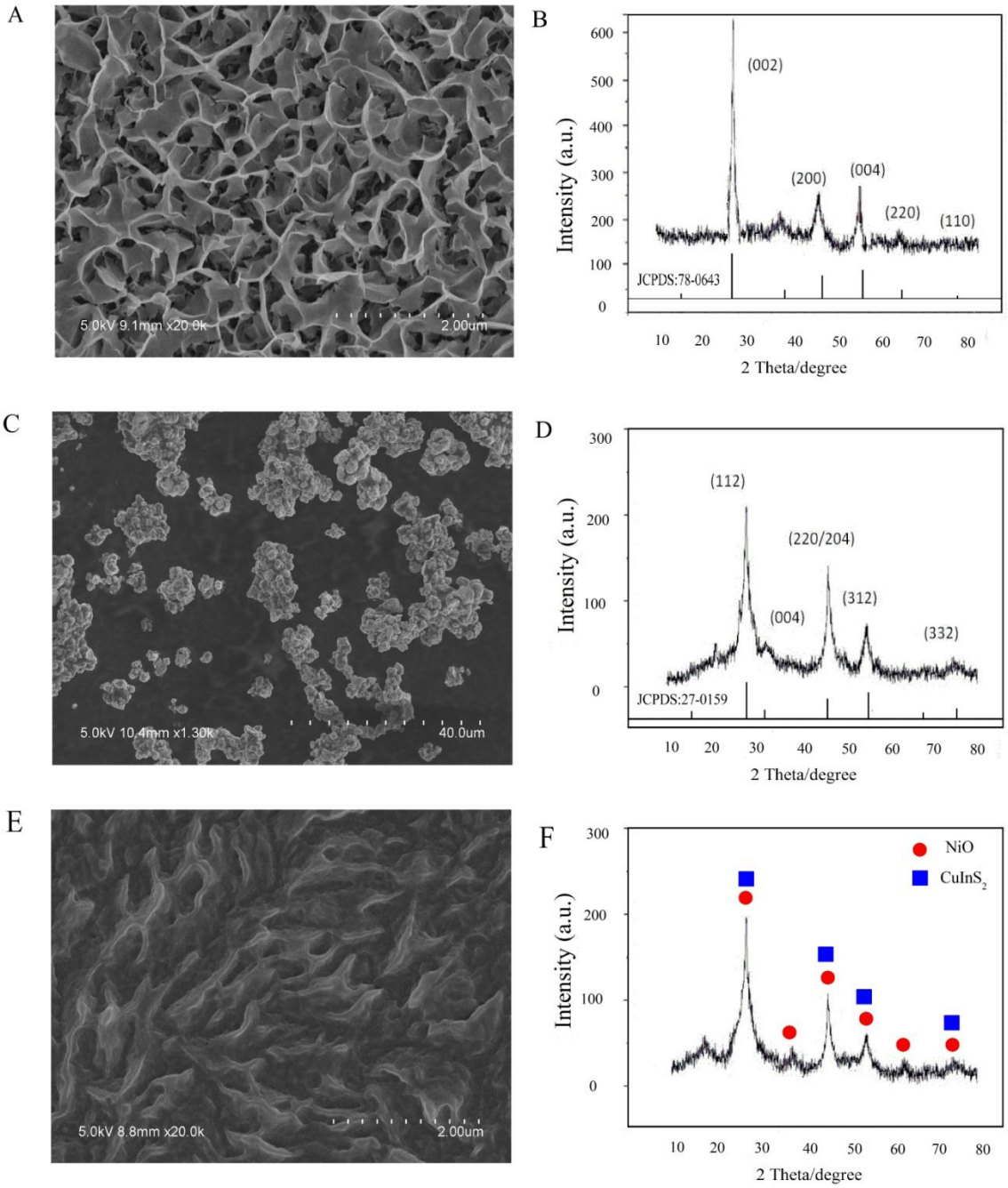

Figure 1 (A) SEM and (B) XRD of NiO porous nanostructure, (C) SEM and (D) XRD of $CuInS_2$ Microspheres，(E) SEM and (F) XRD of $CuInS_2$/NiO electrode.

3.2. Optical Characterization. UV-vis diffuse reflectance spectra were performed for specific optical characterizations. A broad absorption range from 200 to 600 nm was monitored for $CuInS_2$ MSs , indicating its suitability to be a photoactive material under light ($\lambda \geqslant 400$ nm) irradiation (Figure 2A). The UV-vis diffuse reflectance spectra show that NiO electrode hardly had any absorption for visible light due to its broad band gap excitation (Figure 2B), whereas remarkable absorption was seen above 400 nm for $CuInS_2$ MSs/NiO/ITO electrode due to the attachment of sensitization of $CuInS_2$ MSs to NiO film (Figure 2C).

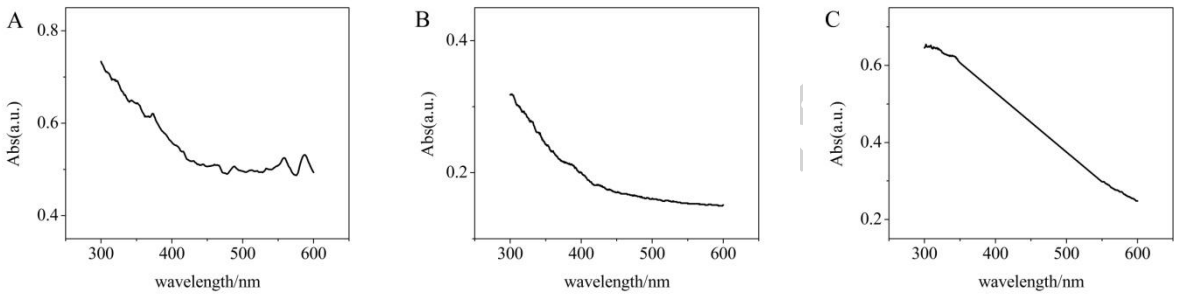

Figure 2 UV-vis spectra of $CuInS_2$(A), NiO/ITO electrode(B) and $CuInS_2$/NiO/ITO electrode(C)

3.3. PEC Characterization. To obtain more enriched information on the light-harvesting properties of the samples, their PEC performances were then disclosed and the results further confirmed the aforementioned measurements. The visible-light-responsibilities were first probed by photocurrent action spectra, and recorded by the measured chronoamperometric I−t curves of NiO/ITO electrode (curve a) and $CuInS_2$/NiO/ITO electrode (curve b) upon visible light illumination (Figure 3A). As shown, upon irradiation, NiO/ITO electrode showed a very small cathodic photocurrent, whereas the $CuInS_2$/NiO/ITO electrode exhibited much enhanced cathodic photocurrent under no biased potential, suggesting the successful sensitization effect and also the good charge transport within the composite. Such a remarkable response should be

attributed to the following reasons: (1) the efficient charge transport and broad visible light absorption of the $CuInS_2$ MSs as the light-sensitive and charge-generating layer. (2) the porous nanoflake of the NiO film could provide high specific area for $CuInS_2$ to load and effective stimulating the electron transport between $CuInS_2$ MSs and NiO. (3) the excellent electrical contact between the crossed NiO and the ITO substrate due to the hydrothermal fabrication, and thus the efficient charge collection by the ITO as photocurrent signal. As shown, upon illumination, the photogenerated electrons transferred from the conduction band (CB) of $CuInS_2$ MSs to the electron acceptors (here in the dissolved oxygen) in the electrolyte, with the photogenerated valence band (VB) holes transfer to the VB of NiO and then easily captured by the ITO electrode, generating a cathodic photocurrent.

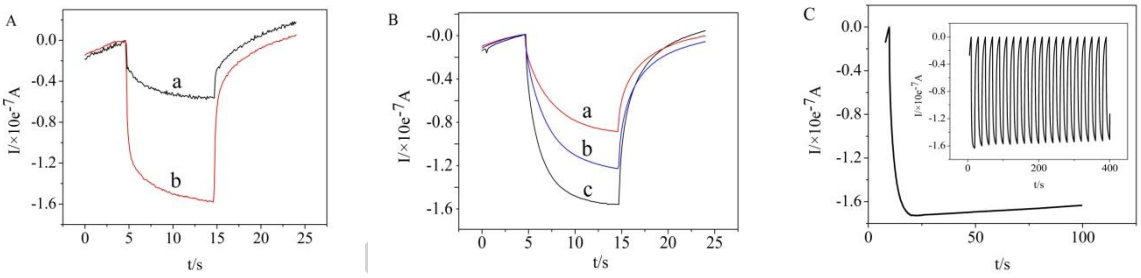

Figure 3 Photocurrent response of NiO/ITO electrode (a) and $CuInS_2$/NiO/ITO electrode(b) in an air-saturated 0.1 M PBS solution (pH 7.4) at 0 V vs Ag/AgCl under visible light irradiation(A). I-t curve of nitrogen saturated (a), H_2O_2 added (b) and air saturated (c) PBS solution(B). Time-based photocurrent response of the as-fabricated $CuInS_2$/NiO/ITO electrode. The inset shows the operational stability test by repeated on/off illumination cycles.

Besides, we also found this photocathode was very sensitive to the ambient oxygen. If the air-saturated electrolyte was deoxygented by purging with highly pure nitrogen, a gradual inhibition could be sensitively produced in the cathodic photocurrent of the hybrid electrode

(Figure 3B). When in the presence of H_2O_2, the photocurrent was rising due to the decomposition of H_2O_2 into O_2. For this photocathode, in continuous illumination test (100 s), the photocurrent intensity decayed slowly because of the consumption of O_2 (Figure 3C). Besides, in the repeated on/off illumination cycles during over 6 min, the photocurrent intensity of the electrode did not show any noticeable decrease (Figure 3C inset). That means the photocathode has good stability in continuous determination process.

3.4. Analytical Performance. Different from the photoanodes that sensitive to the various electron donors (e.g., ascorbic acid, dopamine, cysteine, H_2O_2, etc.), for the photocathodes, the photoinduced electrons would immigrate to their surfaces while the holes transfer to the electrode, resulting in their preferable interactions with electron acceptors (e.g., dissolved O_2) in the electrolyte solution rather than electron donors. Such unique feature endows them with excellent anti-interference ability (enhanced selectivity) against the reductive agents coexisting in biological samples, and hence has immense potential in the field of self-powered PEC sensing. However, to date, quite limited efforts have been exerted on this field. Here we implemented the developed $CuInS_2$/NiO/ITO photocathode along with the sarcosine oxidase (SOx) catalytic events for sarcosine determination. It demonstrated the photocurrent responses in the presence of variable sarcosine concentration at a bias potential of 0.0 V (Figure 4). The cathodic photocurrent decreased steadily with the increased sarcosine concentration, and reached a saturation level at 10 mM sarcosine concentration. This negative correlation between the observed cathodic photocurrent and sarcosine concentration was caused by the competition of the photocathode and SOx toward the dissolved O_2. When the SOx immobilized electrode was exposed to a solution containing sarcosine, the SOx could efficiently catalyze the conversion of

sarcosine into formaldehyde and hydrogen peroxide with the rapid consumption of dissolved oxygen, thus inhibiting the photoinduced electron transfer and thus depressed cathodic photocurrent (Scheme 1). Incidentally, previous reports have demonstrated that the oxygen was much more efficient than hydrogen peroxide during the PEC test. The corresponding derived calibration curve was depicted (Figure 4A inset). It can be seen that the $CuInS_2$/NiO/ITO photocathode showed good linearity in the range of 0.01-1.00 mM for the detection of sarcosine. The limit of detection was 0.008 mM (S/N=3) and the linear regression equation was $I=3.814e^{-8}c-1.122e^{-8}$ with a correlation coefficient of 0.995 (n=6). Common coexisting interfering species such as ascorbic acid (AA), dopamine (DA), L-lysine, L-histidine, urea and glucose were examined. The interference experiments were performed by using sarcosine and interfering species at the same concentration (1.0 mM). The results showed that only sarcosine declined the photocathodic currents (Figure 4B). That means the SOx/$CuInS_2$/NiO/ITO electrode has good selectivity to sarcosine.

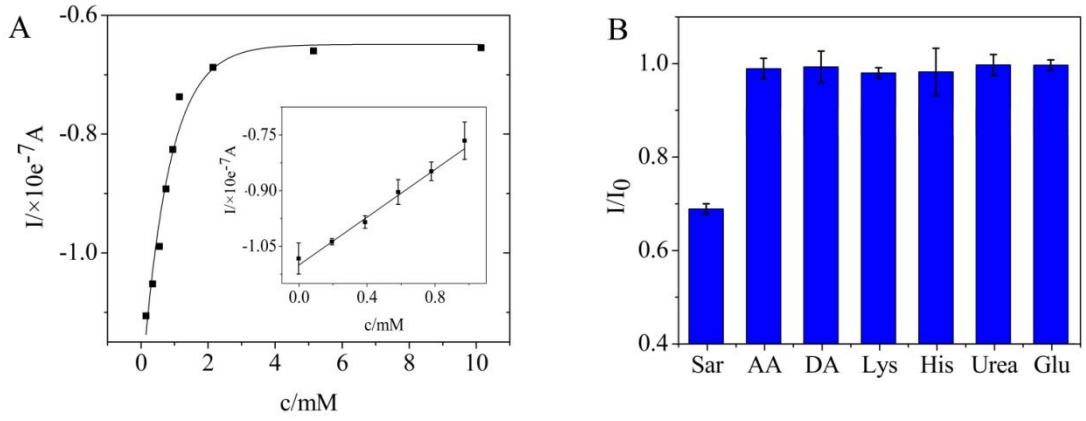

Figure 4 (A) Photocurrent response of the enzyme electrode corresponding to different sarcosine concentration. The inset shows the relationship between photocurrent decrease and sarcosine concentration increase. (B) Photocurrent response of the enzyme electrode corresponding to different substances (1 mM) in 10 mM PBS solution (pH 7.4).

4. Conclusions

In conclusion, this work demonstrated the suitability of the $CuInS_2$/NiO/ITO heterostructure as the photocathode for the SOx-based PEC determination of a biologically important substance of sarcosine. $CuInS_2$ and NiO/ITO were fabricated using hydrothermal methods, respectively, and then coupled to form the heterostructured photocathode, followed by the integration with SOx to prepare the proposed biosensor. In the detection, the O_2-dependent suppression of the cathodic photocurrent can be observed due to the competition for the dissolved O_2 between the O_2-sensitive photocathode and SOx-catalytic reaction for O_2 reduction, thereby a novel and sensitive photocathodic enzymatic sensor was realized and the biosensor exhibited good performance. The linear range for SOx-based electrode was from 0.01 to 1.00 mM. This work displayed the desirable potential of $CuInS_2$-based heterostructured photocathodic enzymatic sensing and was expected to inspire more interests in the design and implementation of numerous other cathodic PEC bioanalytical systems. Further work will focus on the experimental optimization for better performance.

Acknowledgements

This work was supported by the Science and Technology Ministry of China (Grant No. 2016YFA0201200), the National Natural Science Foundation of China (Grant Nos. 21327902, 21475085, 21675080, and 21771107) and the Natural Science Foundation of Jiangsu Province (Grant Nos. BK20161484, BK20170073), and the Fundamental Research Funds for the Central Universities (Grant NO. NE2015003). This work was also supported by a Project Funded by the Priority Academic Program Development of Jiangsu Higher Education Institutions.

REFERENCES

Brown, A.M., Antila, L.J., Mirmohades, M., Sonja, P., Sascha, O., Leif, H., 2016. J. Am. Chem. Soc. 138, 8060-8063.

Dai, W.X., Zhang, L., Zhao, W.W., Yu, X.D., Xu, J.J., Chen, H.Y., 2017. Anal. Chem. 89, 8070-8078.

Fan, G.C., Shi, X.M., Zhang, J.R., Zhu, J.J., 2016. Anal. Chem. 88, 10352-10356.

Gray, N., Zia, R., King, A., Patel, V., Wendon, J., Mcphail, M.J.W., Coen, M., Plumb, R., Wilson, I.D., Nicholson, J.K., 2017. Anal. Chem. 89, 2478-2487.

Guo, Q., Ford, G.M., Hillhouse, H.W., Agrawal, R., 2009. Nano Lett. 9, 3060-3065.

Han, Z.Z., Luo, M., Chen, L., Pan, H., Chen, J.H., 2017. Microchim. Acta 184, 2541-2549.

Huang, W.C., Tseng, C.H., Chang, S.H., Tuan, H.Y., Chiang, C.C., Lyu, L.M., Huang, M.H., 2012. Langmuir 28, 8496-8501.

Jaffar, S.; Nam, K.T.; Khademhosseini, A., Xing, J., Langer, R.S., Belcher, A.M., 2004. Nano Lett. 4, 1421-1425.

Ji, Z.Q., He, M.F., Huang, Z.J., Ozkan, U., Wu, Y.Y., 2013. J. Am. Chem. Soc. 135, 11696-11699.

Jiang, Y.Q., Chen, X.L., Wang, C., Ma, Y.F., 2010. Anal. Chem. 82, 9022-9027.

Kolny, O.J., Weller, H., 2013. Acs Appl. Mater. Inter. 5, 12221-12237.

Kopper, P.H., 1950. J. Gene. Phys.34, 9-17.

Kuo, K.T., Liu, D.M., Chen, S.Y., Lin, C.C., 2009. J. Mater. Chem. 19, 6780-6788.

Lepleux, L., Chavillon, B., Pellegrin, Y., Blart, E., Cario, L., Jobic, S., Odobel, F., 2009. Inorg. Chem. 48, 8245-8250.

Li, L., Coates, N., Moses, D., 2010. J. Am. Chem. Soc. 132, 22-23.

Li, T.L., Teng, H.S., 2010. J. Mater. Chem. 20, 3656-3664.

Mai, L.Q., Yang, F., Zhao Y.L., Xu, X., Xu, L., Luo, Y.Z., 2011. Nature Comm. 2, 381.

Meyer, T.E., Fox, S.D., Issaq, H., J., Xu, X., Chu, L.W., Veenstra, T.D., Hsing, A.W., 2011. Anal. Chem. 83, 5734-5740.

Niklasson, G.A., Granqvist, C.G., 2007. J. Mater. Chem. 17, 127-156.

Ostermann, R., Li, D., Yin, Y.D., Mccann, J.T., Xia, Y.N., 2006. Nano lett. 6, 1297-1302.

Park, S., Kim, S., Kim, H.J., Lee, C.W., Song, H.J., Seo, S.W., Park, H.K., Kim, D.W., Hong, K.S., 2014. J. Hazard. Mater. 275, 10-18.

Peng, Y., Yan, M., Chen, Q.G., Fan, C.M., Zhou, H.Y., Xu, A.W., 2014. J. Mater. Chem. A 2, 8517-8524.

Rebelo, T.S.C.R., Pereira, C.M., Sales, M.G.F., Noronha, J.P., Rodrigues, J.C., Silva, F., Fernandes, M.H., 2014. Anal. Chim. Acta 850, 26-32.

Riedel, M., Goebel, G., Abdelmonem, A.M., Parak, W.J., Lisdat, F., 2013. Chemphychem 14, 2338-2342.

Ruan, Y.F., Zhang, N., Zhu, Y.C., Zhao, W.W., Xu, J.J., Chen, H.Y., 2017. Anal. Chem. 89, 7869-7875.

Shen, G.Z., Chen, D., Lee, C.J., 2006. J. Phy. Chem. B 110, 15689-15693.

Sreekumar, A., Poisson, L.M., Rajendiran, T.M. et al., 2009. Nature 457, 910-914.

Surbhi, C., Sumant, U., Pushpendra, K., Nirupama, S., Vibha, R.S., Rohit, S., Sahab, D., 2012. Int. J. Hydrogen Energy 37, 18713-18730.

Takahashi, Y., Tatsuma, T., 2010. Nanoscale 2, 1494-1499.

Tsai, G.C., Lane, H.Y., Yang, P.C., Chong, M.Y., Lange, N., 2004. Biol. Psychiatry 55, 452-456.

Valenti, G., Rampazzo, E., Biavardi, E. et al., 2015. Faraday Discuss. 185, 299-309.

Wang, C.H., Shao, C.L., Zhang, X.T., Liu, Y.C., 2009. Inorg. Chem. 48, 7261-7268.

Wang, G.L., Gu, T.T., Dong, Y.M., Wu, Y.M., Li, Z.J., 2015. Electrochem. Commun. 61, 117-120.

Wang, G.L., Liu, K.L., Dong, Y.M., Wu, X.M., Zhang, C., 2014. Biosens. Bioelectro. 62, 66-72.

Wang, G.L., Liu, K.L., Shu, J.X., Gu, T.T., Wu, X.M., Dong, Y.M., Li, Z.J., 2015. Biosens. Bioelectro. 69, 106-112.

Wang, G.L., Shu, J.X., Dong, Y.M., Wu, X.M., Zhao, W.W., Xu, J.J., Chen, H.Y., 2015. Anal. Chem. 87, 2892-2900.

Wang, W.W., Wu, Z.L., Dai, Z.L., Yang, Y., Wang, J.J., Wu, G.Y., 2013. Amino Acids 45, 463-477.

Willsey, G.G., Wargo, M.J., 2015. J. Bacteriology 198, 301-310.

Wyss, M., Kaddurah, D.R., 2000. Physiol. Rev. 80, 1107-1213.

Xue, Z.H., Wang, H., Rao, H.H., He, N., Wang, X.F., Liu, X.H., Lu, X.Q., 2017. Talanta 167, 666-671.

Yang, H.B., Guai, G.H., Guo, C.X., Song, Q.L., Jiang, S.P., Wang, Y.L., Zhang, W., Li, C.M., 2011. J. Phys. Chem. C 115, 12209-12225.

Yong, K.T., Roy, I., Hu, R., Ding, H., Cai, H.X., Zhu, J., Zhang, X.H., Bergey, E.J., Prasad, P.N., 2010. Integr. Biol. 2, 121-129.

Yue, W.J., Han, S.K., Peng, R.X., Shen, W., Geng, H.W., Wu, F., Tao, S.W., Wang, M.T., 2010. J. Mater. Chem. 20, 7570-7578.

Zang, Y., Lei, J.P., Hao, Q., Ju, H.X., 2016. Biosens. Bioelectro. 77, 557-564.

Zhang, D.F., Sun, L.D., Jia, C.J., Yan, Z.G., Yan, C.H., 2005. J. Am. Chem. Soc. 127, 13492-13493.

Zhang, N., Ma, Z.Y., Ruan, Y.F., Zhao. W.W., Xu J.J., Chen H.Y., 2016. Anal. Chem. 88, 1990-1994.

Zhang, N., Zhang, L., Ruan, Y.F., Zhao, W.W., Xu, J.J., Chen, H.Y., 2017. Biosens. Bioeletro. 94, 207-218.

Zhang, Z.H., Wang, P., 2012. J. Mater. Chem. 22, 2456-2464.

Zhao. W.W., Xu, J.J., Chen, H.Y., 2014. Chem. Rev. 114, 7421-7441.

Zhou, W.J., Yin, Z.Y., Du, Y.P., Huang, X., Zeng, Z.Y., Fan, Z.X., Liu, H., Wang, J.Y., Zhang, H., 2013. Small 9, 140-147.

Zhu, G.X., Liu, Y.J., Xu, H., Chen, Y., Shen, X.P., Xu, Z., 2012. Crystengcomm 14, 719-725.

Zhu Y.C., Xu, F., Zhang, N., Zhao, W.W., Xu, J.J., Chen, H.Y., 2017. Biosens. Bioelectro. 293-298.

Highlights

- $CuInS_2$/NiO/ITO hierarchical heterostructure was fabricated.
- It was then applied for the novel photocathodic sarcosine bioanalysis.
- The proposed format could serve as a general basis for $CuInS_2$-based cathodic PEC biosensors.